HHS Public Access

Author manuscript

*IEEE Int Conf Robot Autom*. Author manuscript; available in PMC 2015 July 06.

Published in final edited form as:

*IEEE Int Conf Robot Autom*. 2015 May ; 2015: 5378–5383. doi:10.1109/ICRA.2015.7139950.

# Tendons, Concentric Tubes, and a Bevel Tip: Three Steerable Robots in One Transoral Lung Access System

**Philip J. Swaney**[1] **[Student Member, IEEE]**, **Arthur W. Mahoney**[1] **[Member, IEEE]**, **Andria A. Remirez**[1] **[Student Member, IEEE]**, **Erik Lamers**[1], **Bryan I. Hartley**[2], **Richard H. Feins**[3], **Ron Alterovitz**[4] **[Member, IEEE]**, and **Robert J. Webster III**[1] **[Senior Member, IEEE]**

Philip J. Swaney: philip.j.swaney@vanderbilt.edu; Ron Alterovitz: ron@cs.unc.edu; Robert J. Webster: robert.webster@vanderbilt.edu

[1]Mechanical Engineering at Vanderbilt University, Nashville, TN 37235, USA

[2]Department of Radiology and Radiological Sciences, Vanderbilt University, Nashville, TN 37235, USA

[3]Division of Cardiothoracic Surgery, Department of Surgery, University of North Carolina School of Medicine, Chapel Hill, NC 27599, USA

[4]Department of Computer Science, University of North Carolina at Chapel Hill, Chapel Hill, NC 27599, USA

## Abstract

Lung cancer is the most deadly form of cancer, and survival depends on early-stage diagnosis and treatment. Transoral access is preferable to traditional between-the-ribs needle insertion because it is less invasive and reduces risk of lung collapse. Yet many sites in the peripheral zones of the lung or distant from the bronchi cannot currently be accessed transorally, due to the relatively large diameter and lack of sufficient steerablity of current instrumentation. To remedy this, we propose a new robotic system that uses a tendon-actuated device (bronchoscope) as a first stage for deploying a concentric tube robot, which itself is a vehicle through which a bevel steered needle can be introduced into the soft tissue of the lung outside the bronchi. In this paper we present the various components of the system and the workflow we envision for deploying the robot to a target using image guidance. We describe initial validation experiments in which we puncture ex vivo bronchial wall tissue and also target a nodule in a phantom with an average final tip error of 0.72 mm.

## I. Introduction

Lung cancer kills more people than any other form of cancer, with more than 150,000 Americans dying from it each year [1]. Survival is highly dependent on early diagnosis and treatment [2], [3]. Current imaging techniques enable the detection of small nodules, but definitive diagnosis requires biopsy. The least invasive and most common procedures for biopsy are percutaneous and transoral bronchoscopic biopsy, both of which have drawbacks. Percutaneous techniques can access the peripheral lung, but require puncture of the pleura, which may result in pneumothorax (lung collapse) up to 25% of the time [4], which is a serious enough complication that some patients will die from it. Bronchoscopic methods do not puncture the pleura (so the risk of pneumothorax is low) but the majority of the lung is

inaccessible, due to either the diameter of the bronchi being too small to traverse or the target not being directly accessible from the bronchial tree.

To bring the benefits of transoral access to patients with peripheral lung nodules, our system (Fig. 1(a)) integrates a standard tendon-actuated bronchoscope with a concentric tube robot and a bevel tip steerable needle (Fig. 1(b)). In order to enable bronchoscopic access to a target, the device must enter the airway via the nose or mouth, navigate the bronchial tubes to a site near the desired target, pierce and travel through the bronchial wall, and steer through lung tissue to the target (Fig. 1(c)). Achieving this requires multiple steering mechanisms. Bronchoscopes are standard medical devices that consist of a flexible shaft with a tendon-driven tip that bends into a circular shape when the tendons are pulled by levers on the handle. For an overview of tendon operated devices and constant curvature robots in general see [5]. Concentric tube robots consist of a series of pre-curved, superelastic tubes that translate and rotate inside one another to create curvilinear collective motion. Mechanics-based models for them have been derived [6], [7], and these robots have been applied in a variety of surgical contexts (for a review of both, see [8]). Deploying a concentric tube robot through an endoscope is a relatively new idea [9], [10], and it has been shown that they can augment the dexterity of standard endoscopes. However, concentric tube robots have not previously been used to deploy bevel tip steerable needles, and the three steering methods have not previously been combined into a single system. Bevel tip steerable needles [11] harness the assymmetry of a wedge-like bevel tip to bend controllably as they pass through tissue. Such steerable needles have been the subject of much recent research in control, motion planning, and design (see [12] and [13] for reviews). In this paper we use a new variant of the bevel tip needle called a flexure tip needle [14], which is less damaging to the tissue than alternative high-curvature designs.

## II. System Concept

We envision the system, shown in Fig. 2, being used for lung biopsy and therapy delivery under either fluoroscopic guidance, real-time computed tomography (CT), or via magnetic tracking combined with preoperative CT or magnetic resonance images. The deployment of the three stages of the device is illustrated in Fig. 1(c). At a more granular level, the intended insertion workflow is as follows:

1. The surgeon deploys the bronchoscope transorally using standard practices (Note: this step could potentially be robotized in the future, but it may be simpler to have the surgeon do it manually). An Olympus BF 1T30 bronchoscope was used for this work.
2. The concentric tube robot is deployed through the bronchoscope tool port to reach the bronchial wall.
3. A sharp nitinol wire connected to a spring-loaded mechanism at the rear of the concentric tube robot is deployed through the concentric tube robot and used to create an opening in the bronchial wall. After the opening is created, the wire and puncture mechanism are removed.

4. The concentric tube robot deploys its second tube a short distance through the bronchial wall, aiming its tip approximately toward the target.
5. The steerable needle is deployed through the concentric tube robot and delivered under closed-loop control to the desired target.
6. The surgeon advances a coaxial access tube through the bronchoscope and over the steerable needle, creating an access channel to the target through which a biopsy can be collected or a therapeutic agent can be deposited. Note that in this paper we are focused on targeting, and leave the therapy delivery step (step (6)) to future work, as prior needle steering papers have done (see [12], [13]).

The following sections will elaborate on aspects of this workflow and the mechanical devices and algorithms used to achieve the various steps.

## III. From Bronchoscope Tip to Bronchi Exit

### A. Within The Bronchi

In step 2 of the workflow presented in Sec. II, the outer tube of the two-tube concentric tube robot (concentric tube robot parameters given in Table I) is deployed from the bronchoscope tip to the desired site on the bronchial wall where the surgeon wishes to exit the bronchi and begin traveling through the soft tissue (called “parenchyma”) of the lung. Typically, the surgeon will deploy the bronchoscope as deeply as possible before deploying the other steering devices, and the bronchi diameter will not be much larger than the diameter of the bronchoscope itself. This motivates the need for the concentric tube robot to bend toward the wall, to enable the puncturing needle to approach the wall as perpendicularly as possible, as shown in Fig. 3. The complete kinematics of the concentric tube robot are given in [6], [7]. Here, since only one tube extends from the bronchoscope, the simplified model given in [9] may be used.

### B. Exiting the Bronchi

Next, (step 3 in Sec. II) we deploy the sharp nitinol wire (0.78 mm OD) through the concentric tube robot. Since the wall of the bronchi is made from relatively tough cartilage rings and connective muscular tissue, it is necessary to apply a short rapid motion with a sharp needle to puncture it, thereby creating a port through which the concentric tube robot can pass. To accomplish this, we designed a spring-loaded mechanical system [15] capable of imparting the required velocity and force to the needle. The mechanism is shown in Figure 4. It operates by translating a plunger attached to the nitinol wire backward until the spring is fully compressed. The spring can then be released from the plunger using a lever, propelling the nitinol wire forward a short distance. The wire transmits this motion all the way through the bronchoscope and concentric tube robot to the bronchial wall. This causes the needle to puncture the bronchial wall. Puncture depth can be manually adjusted by the surgeon by setting the initial position of the needle tip within the concentric tube robot (it need not be initially flush with the tip of the concentric tubes). When deployed, the puncture needle does not appreciably change the overall shape of the bronchoscope or concentric tube robot because it is approximately 5 times less stiff than the concentric tube robot.

### C. Establishing the Initial Bevel Needle Pose

Now that a port has been created in the bronchial wall, the concentric tube robot can pass through it and establish the initial pose of the bevel steered needle (Sec. II, step 4). The concentric tube robot does this by advancing its second tube through the first and rotating it to aim its tip in the general direction of the target (see Figs. 1 and 5). The goal of this process is to set the initial pose of the bevel steered needle such that the target lies within the needle's workspace, and ideally toward the workspace center. Bevel tip steerable needles have a roughly "trumpet shaped" workspace for clinically realistic arc lengths, which is bounded by the maximum curvature achievable with the needle.

## IV. Steering Through Parenchyma to the Target

We use the flexure tip steerable needle design [14] to steer through soft tissue toward the target. Reviewing the design described in [14], the needle consists of three parts: a flexible needle shaft, a beveled needle tip, and a flexure to join the shaft and the needle tip. All three components are made from nitinol. Upon insertion into tissue, the asymmetric bevel produces a force on the needle tip that causes the flexure to bend and the needle to follow a curved trajectory through tissue. The flexure element causes the steerable needle to achieve relatively high curvatures as it passes through tissue, yet cause minimal tissue damage because the flexure will straighten as the needle is axially rotated.

The needle shaft used for our system validation experiment has an OD of 0.8 mm and an ID of 0.6 mm. The bevel tip has an OD of 1.16 mm, a slightly larger OD than the needle shaft, in order to house a six-degree-of-freedom magnetic tracking sensor (NDI Aurora, Canada). The bevel tip itself has a length of 4 mm and a bevel angle of approximately 15°. The flexure is comprised of three 0.125 mm nitinol wires positioned side by side along the longitudinal axis of the needle shaft (see Fig. 1(b)). The length of the entire needle is 1.21 m.

We use the sliding mode controller of Rucker et al. [16] to drive the needle to the tumor target. The control strategy has a number of useful features. First, it does not require initial knowledge of model parameters (in particular needle curvature), it produces bounded actuator velocities, and it is not computationally intensive. Furthermore, it can be proven that the control law will cause the system to converge to desired workspace targets in finite time. The control law has been previously validated in the contexts of reaching target points, trajectory following, and targeting objects moving within the tissue media (e.g. due to respiration).

## V. Experimental Evaluation

To illustrate the use of our system for accessing targets outside of the bronchial tubes via a flexible bronchoscope, we performed a bronchial wall puncture experiment and a phantom validation study (see Fig. 6 for experimental setup). For both experiments, we created a model bronchial tree from clear PVC plastic that includes three generations of phantom bronchi. Each bronchial tube is smaller than the one it extends from, mimicking the structure of the human lung. An 8 mm diameter access hole was placed in the side wall of the third and smallest bronchial tube to allow the concentric tubes and steerable needle to pass out of

the bronchial tube. In order to accurately test the capability of our puncture mechanism, we dissected a porcine lung and removed a portion of the primary bronchial tube, which was then wrapped around our phantom tube and placed over the 8 mm hole, enabling us to test the puncture mechanism with ex vivo tissue.

The concentric tube robot and puncture needle were then loaded into the bronchoscope. They were loaded from the tip of the bronchoscope backward, to ensure that the curved sections of the concentric tube robot would not have to pass through the sharp bends in the bronchoscope handle and potentially become plastically deformed. At the end of the loading procedure, the base of the concentric tube robot and the puncture needle extended out of the port on the bronchoscope handle, and could be grasped by the robotic actuation unit and the puncture mechanism. A telescoping support sheath was used to prevent buckling in the portion of the puncture needle located behind the bronchoscope handle. The tips of the concentric tube robot and puncture needle were retracted fully within the bronchoscope such that their tips rested just behind the start of the tendon-actuated steering section at the distal end of the bronchoscope, which did not result in any plastic deformation of the tubes. The bronchoscope was then guided through the phantom bronchial tree using the tendon-actuated tip of the bronchoscope until it reached the ex vivo porcine bronchial wall, at which point the concentric tube robot and puncture needle were extended to the bronchial wall and the puncture needle was fired and successfully created a port in the bronchial wall. This experiment demonstrated the ability of the puncture mechanism to perform its function in a realistic setting.

Next, in order to test the steering capabilities of our system, the flexure tip needle was loaded into the concentric tube robot and bronchoscope in the same manner as the puncture needle. The ex vivo tissue was removed, and the bronchial tree embedded in a clear gelatin phantom made from 10% by weight Knox gelatin (Kraft Foods Global Inc., USA), used as a surrogate for lung tissue surrounding the bronchi (see Fig. 6). The bronchoscope was then guided through the phantom bronchial tree using the tendon-actuated tip of the bronchoscope until it reached the exit hole in the bronchial tree. The concentric tube robot was deployed within the lumen in the direction necessary to align the steerable needle toward the target, and then advanced into the gelatin. Finally, the bevel tip needle was advanced and steered through the simulated parenchyma to the target using the sliding mode controller under magnetic tracker feedback. The average tip error in three trials was 0.72 mm. The results of each trial are shown in Fig. 7.

## VI. Discussion

The system and workflow presented in this paper for targeting suspicious lung nodules is a novel robotic approach with the potential to save lives by enabling earlier-stage definitive diagnosis of lung cancer. By avoiding needle insertion through the skin into the lung, our approach has the potential to reduce the risk of pneumothorax (lung collapse), which is a serious and life threatening complication for patients with co-morbidities or reduced lung function. Rather than waiting to see if a tumor grows over time in medical images, our system would give physicians the option of obtaining a definitive diagnosis when a suspicious nodule is first detected, for a broader class of patients. The system was able to

accurately target nodules in a phantom validation experiment. However, there remain many challenges and avenues for future work with this system.

First, our model for the parenchyma is gelatin, which does not perfectly match the material properties and inhomogeneity of lung tissue. It will be necessary in the future to carefully tune the steerable needle's properties (shaft stiffness, flexure stiffness, bevel angle, etc.) to achieve the desired curvature in lung tissue. This challenge is not unique to our work – a large number of prior bevel steering papers have used gelatin phantoms, and the feasibility of subsequently tuning needle properties to a variety of tissues (e.g. brain [17], liver [18], kidney [18], muscle [11]) has been previously established.

A challenge we overcame while creating the system described in this paper was inserting tubes through the working channel in a standard clinical bronchoscope. In order to pass the nitinol tubes through the bronchoscope, we first inserted a thin-walled PTFE sheath that ran the length of the bronchoscope working channel. This sheath allowed the tubes to navigate the tight corner in the channel within the handle of the bronchoscope where the side port turns and begins to run along the shaft of the bronchoscope. This turn was sufficiently high curvature that the tubes slightly plastically deformed when passing through it. Another benefit of the sheath is that it prevented any sharp edges on the tubes from scoring the interior of the bronchoscope channel.

Another challenge worthy of note is that due to the length of the bronchoscope (67 cm) and the length of the steerable needle (121 cm), significant torsional windup due to friction occurred in the steerable needle shaft. We addressed this challenge by incorporating a 6 degree-of-freedom (DoF) magnetic tracking sensor, which is larger in diameter than available 5 DoF sensors. In future work, involving the integration of a biopsy collection/ therapy delivery tube, it may be useful to use a 5 DoF tracking coil (or even medical images) and incorporate a torsional observer like the one described in [19]. The shape of the bronchoscope will also affect the torsion in the steerable needle, and it is unclear whether this effect will need to be explicitly modeled.

One must also be aware that depending on the diameter and number of tubes/wires passing through the bronchoscope, they may stiffen the tendon-actuation section of the bronchoscope to varying degrees. A solution to this challenge that we employed in this paper was to retract all tubes and the needle such that their tips do not pass into the bending tip of the bronchoscope during bronchoscope deployment into the lung. Another possible approach would be laser machining the tubes to decrease their bending stiffness, as was done for other purposes in [20].

It is also important to consider concentric tube robot elastic stability when using robots of this type. Algorithms are available to design bifurcation-free concentric tube robots [21], [22]. Our approach in this paper was to make the length of the curved section of the inner tube as short as possible, so that the curved section can be fully extended from the outer tube, before rotating. This will require either full deployment in the open lumen of both tubes, or some tissue stretching in the parenchyma, and future experiments will be needed to determine whether the stretching is substantial enough to damage lung tissue and if the tube

has enough torsional stiffness to deflect the tissue. It is also possible that a future system will be able to dispense with the inner curved tube altogether if the bevel steered needle exhibits sufficient curvature in the parenchyma.

Lastly, while the workflow we propose in this paper will certainly require some adaptation by clinical personnel, we do not foresee this as a major challenge. The reason is that our proposed workflow is similar to existing image-guided lung biopsy procedures that use bronchoscope deployed, magnetically tracked (but not steerable in parenchyma) instruments [23].

## VII. Conclusion

In conclusion, we note that lung cancer is an important healthcare challenge that will only grow in importance in the future. This is because the U.S. Preventative Services Task Force has recently begun recommending yearly low-dose CT screening for all individuals between the ages of 55 and 80 who have at least a 30 pack-year smoking history and are current smokers or who have quit in the last 15 years [24]. This will result in an estimated 1–2 million *more* small suspicious nodules discovered each year, many of which will need to be biopsied. The robotic system and envisioned workflow (see Fig. 8) described in this paper are a step toward addressing this significant clinical need. We demonstrated its ability to puncture through ex vivo porcine wall tissue and to reach targets in phantom tissue with an average tip error of 0.72 mm. The new approach we have proposed minimizes the risk of pneumothorax by deploying transorally through a clinical flexible bronchoscope. It is the first system with the potential to steerably biopsy peripheral lung regions deep in the parenchyma, via a transoral approach.

## Acknowledgments

This material is based upon work supported by the National Institutes of Health under award R21 EB017952 and the National Science Foundation under award IIS-1054331 as well as two NSF Graduate Research Fellowships. Any opinions, findings, and conclusions or recommendations expressed in this material are those of the authors and do not necessarily reflect the views of the NIH or the NSF.

## References

1. American Cancer Society. Tech Rep. American Cancer Society; 2010. Cancer facts & figures 2010.
2. The International Early Lung Cancer Action Program Investigators. Survival of patients with stage I lung cancer detected on CT screening. The New England Journal of Medicine. 2006; 355(17):1763–1771. [PubMed: 17065637]
3. Horner, MJ.; Ries, LAG.; Krapcho, M.; Neyman, N.; Aminou, R.; Howlader, N.; Altekruse, SF.; Feuer, EJ.; Huang, L.; Mariotto, A.; Miller, BA.; Lewis, DR.; Eisner, MP.; Stinchcomb, DG.; Edwards, B. SEER cancer statistics review, 1975–2006. National Cancer Institute; Bethesda, MD: 2009. Available: http://seer.cancer.gov/csr/
4. Wang Memoli JS, Nietert PJ, Silvestri GA. Meta-analysis of guided bronchoscopy for the evaluation of the pulmonary nodule. Chest. 2012; 142(2):385–393. [PubMed: 21980059]
5. Webster RJ III, Jones BA. Design and kinematic modeling of constant curvature continuum robots: a review. International Journal of Robotics Research. 2010; 29:13.
6. Rucker DC, Jones BA, Webster RJ III. A geometrically exact model for externally loaded concentric tube continuum robots. IEEE Transactions on Robotics. 2010; 26(5):769–780. [PubMed: 21566688]

7. Dupont PE, Lock J, Itkowitz B, Butler E. Design and control of concentric-tube robots. IEEE Transactions on Robotics. 2010; 26(2):209–225. [PubMed: 21258648]
8. Gilbert, HB.; Rucker, DC.; Webster, RJ, III. Concentric tube robots: state of the art and future directions. Springer Tracts in Advanced Robotics; 16th International Symposium on Robotics Research; 2013. In Press
9. Hendrick, RJ.; Herrell, SD.; Webster, RJ, III. A multi-arm hand-held robotic system for transurethral laser prostate surgery. IEEE International Conference on Robotics and Automation; 2014. p. 2850-2855.
10. Butler, E.; Hammond-Oakley, R.; Chawarski, S.; Gosline, A.; Codd, P.; Anor, T.; Madsen, J.; Dupont, P.; Lock, J. Robotic neuro-endoscope with concentric tube augmentation. IEEE/RSJ International Conference on Intelligent Robots and Systems; 2012. p. 2941-2946.
11. Webster RJ III, Kim JS, Cowan NJ, Chirikjian GS, Okamura AM. Nonholonomic modeling of needle steering. The International Journal of Robotics Research. 2006; 25(5–6):509–525.
12. Abolhassani N, Patel RV, Moallem M. Needle insertion into soft tissue: a survey. Medical Engineering & Physics. 2007; 29(4):413–431. [PubMed: 16938481]
13. Reed KB, Majewicz A, Kallem V, Alterovitz R, Goldberg K, Cowan NJ, Okamura AM. Robot-assisted needle steering. IEEE Robotics and Automation Magazine. 2011; 18(4):35–46. [PubMed: 23028210]
14. Swaney PJ, Burgner J, Gilbert HB, Webster RJ III. A flexure-based steerable needle: high curvature with reduced tissue damage. IEEE Transactions on Biomedical Engineering. 2013; 60:906–909. [PubMed: 23204267]
15. Lamers, EP.; Remirez, AA.; Swaney, PJ.; Webster, RJ, III. A bronchial puncture mechanism for transoral access to the lung parenchyma. Design of Medical Devices Conference; 2015. Accepted
16. Rucker DC, Das J, Gilbert HB, Swaney PJ, Miga MI, Sarkar N, Webster RJ III. Sliding mode control of steerable needles. IEEE Transactions on Robotics. 2013; 29:1289–1299. [PubMed: 25400527]
17. Minhas, D.; Engh, J.; Riviere, C. Testing of neurosurgical needle steering via duty-cycled spinning in brain tissue in vitro. International Conference of the IEEE Engineering in Medicine and Biology Society; 2009. p. 258-261.
18. Majewicz A, Marra S, van Vledder M, Lin M, Choti M, Song D, Okamura A. Behavior of tip-steerable needles in ex vivo and in vivo tissue. IEEE Transactions on Biomedical Engineering. 2012; 59(10):2705–2715. [PubMed: 22711767]
19. Swensen J, Lin M, Okamura A, Cowan N. Torsional dynamics of steerable needles: modeling and fluoroscopic guidance. IEEE Transactions on Biomedical Engineering. 2014; 61(11):2707–2717. [PubMed: 24860026]
20. Kim, J-S.; Lee, D-Y.; Kim, K.; Kang, S.; Cho, K-J. Toward a solution to the snapping problem in a concentric-tube continuum robot: grooved tubes with anisotropy. IEEE International Conference on Robotics and Automation; 2014. p. 5871-5876.
21. Hendrick, RJ.; Gilbert, HB.; Webster, RJ, III. Designing snap-free concentric tube robots: a local bifurcation approach. IEEE International Conference on Robotics and Automation; 2015. Accepted
22. Xu, R.; Atashzar, SF.; Patel, RV. Kinematic instability in concentric-tube robots: modeling and analysis. IEEE International Conference on Biomedical Robotics and Biomechatronics; 2014. p. 163-168.
23. SuperDimension. SuperDimension i-Logic System. 2010. Available: http://www.superdimension.com
24. Moyer VA. Screening for lung cancer: U.S. preventive services task force recommendation statement. Annals of Internal Medicine. 2014; 160(5):330–338. [PubMed: 24378917]

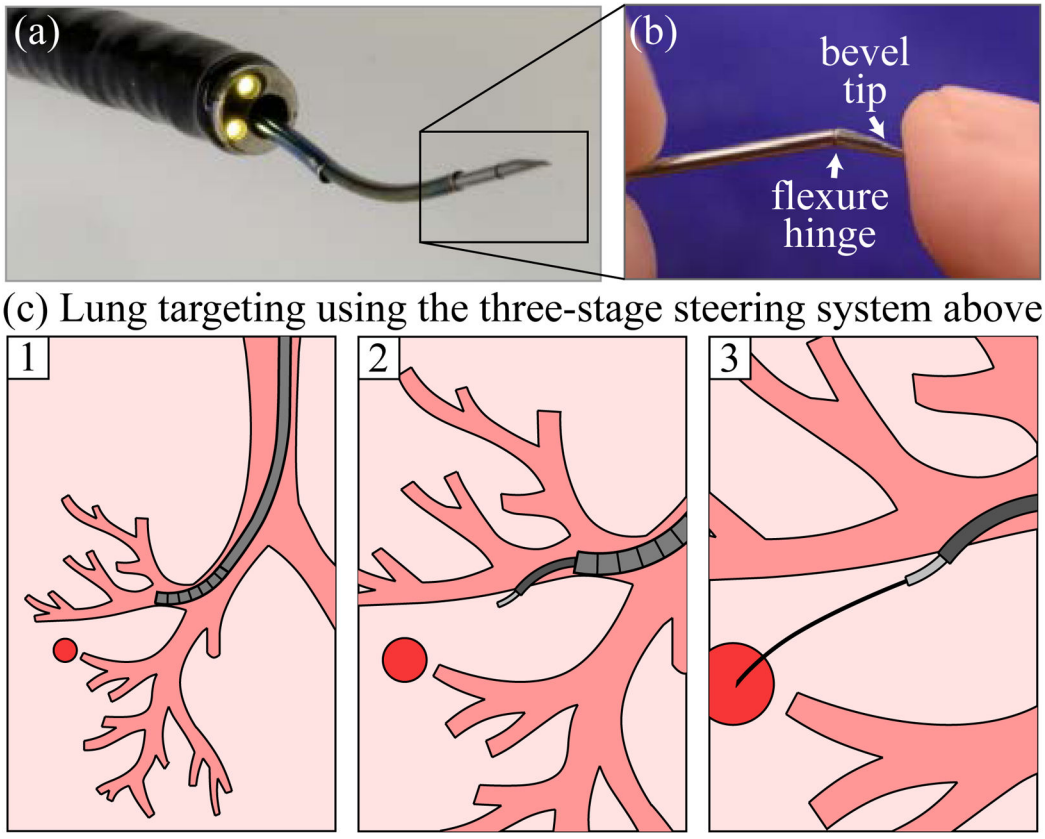


**Fig. 1.**

(a) Our combined bronchoscope, concentric tube robot, and bevel steered needle robot, (b) closeup of bevel tip, (c) steps in deployment involve: (1) deploying the bronchoscope (2) deploying the concentric-tube robot to the bronchial wall, puncturing through it, and entering the parenchyma, and (3) steering the bevel-tip needle to the target under closed-loop control.

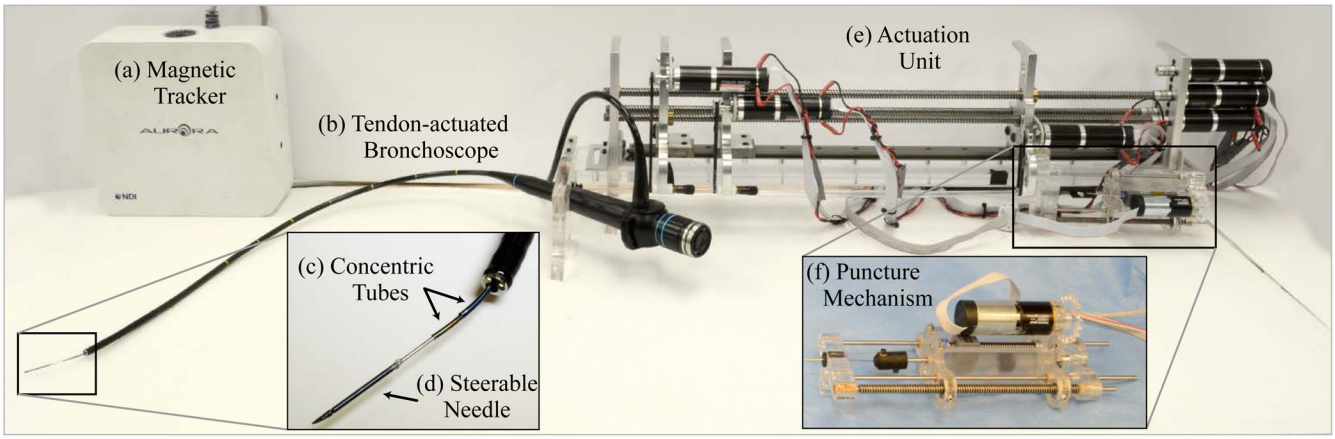


**Fig. 2.**

The components of the three-stage steering system developed in this work are shown. The system includes a (a) magnetic tracking system, (b) tendon-actuated flexible bronchoscope, (c) concentric tube robot, (d) steerable needle, (e) an actuation unit, and a (f) puncture mechanism.

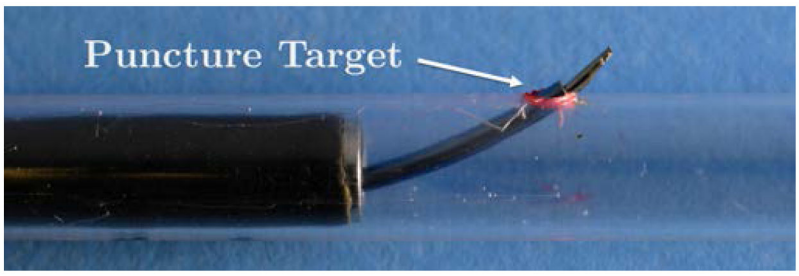


**Fig. 3.**

The concentric tube robot is used to deliver the puncture needle to the bronchial wall. This is needed because often the surgeon will deliver the bronchoscope as deep as possible into the lung, where the bronchoscope's working channel is constrained to be coaxial with the bronchial tube.

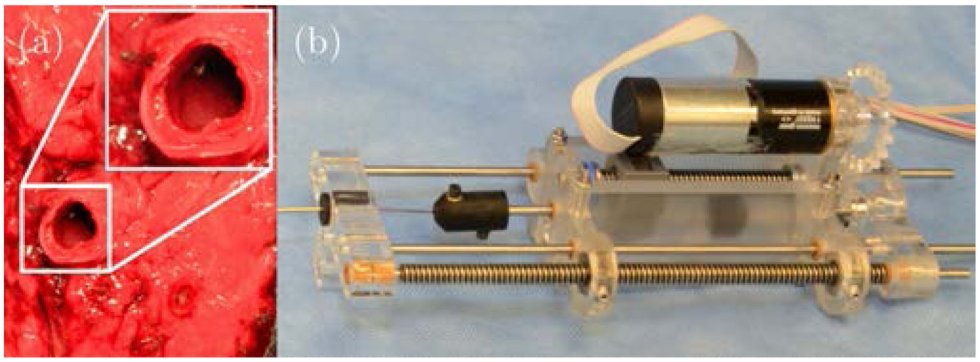


**Fig. 4.**

(a) Puncturing of the bronchial wall in ex vivo porcine lung using the puncture mechanism. The puncture needle was positioned against a sample of ex vivo porcine bronchial wall before firing the puncture needle. (b) Detailed view of the puncture mechanism.

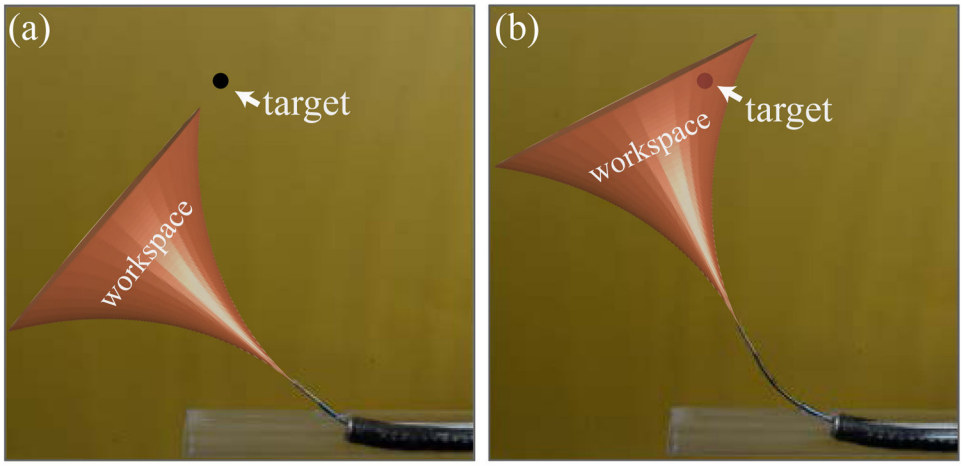


**Fig. 5.**

The second task of the concentric tube robot is to align the workspace of the steerable needle such that the target nodule is within the reachable workspace of the needle. An example of aligning the steerable needle workspace by changing the initial tangent angle of the needle is shown above.

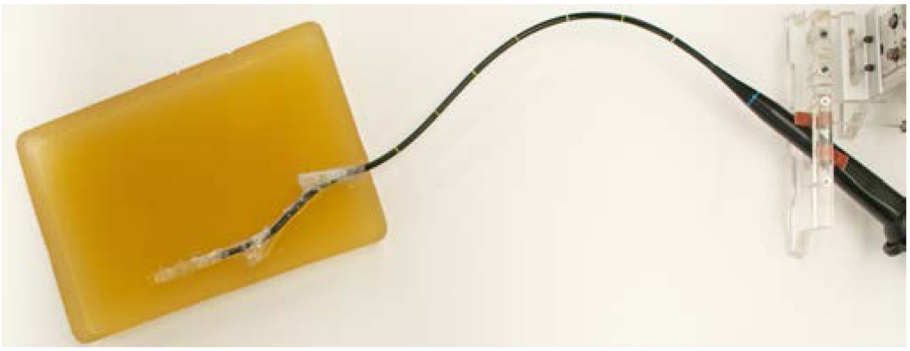

**Fig. 6.**

The experimental setup used for the phantom validation study consisted of a phantom bronchial tree (made from plastic tubes) that was embedded in phantom parenchyma (gelatin).


**Fig. 7.**

The three-stage steering system deployed to three separate targets in the phantom. The tip error for each of the three runs was (a) 1.3 mm, (b) 0.5 mm, and (c) 0.2 mm.

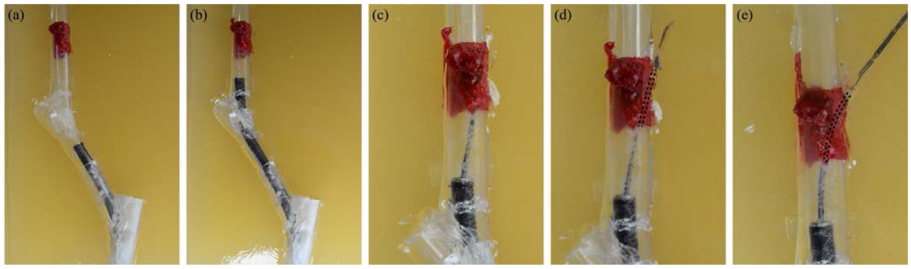


**Fig. 8.**

The proposed lung targeting workflow is demonstrated. First, (a),(b) the endoscope is inserted through the phantom bronchial tube to the puncture site. Then, (c) the concentric tube robot delivers the needle tip to the bronchial wall and (d) punctures through the wall. Finally, (e), the concentric tube robot is deployed to aim the steerable needle toward the target, after which the bevel steered needle is deployed (see Fig. 7).

**TABLE I**

Concentric Tube Parameters Used

| | Outer Tube | Inner Tube |
|---|---|---|
| Outside Diameter (mm) | 1.38 | 1.14 |
| Inside Diameter (mm) | 1.29 | 0.97 |
| Radius of Curvature (mm) | 25.4 | 17.8 |
| Curved Length (mm) | 55 | 27 |
| Straight Length (mm) | 735 | 833 |